

Leveraging Machine Learning for Autonomous Ultrasonic Mitigation of Harmful Algal Blooms Along the Pacific Coast

Varun Rao*
Mission San Jose High School
Fremont, USA
varrao23@gmail.com

Sajeev Magesh*
Dublin High School
Dublin, USA
sajeevmagesh123@gmail.com

Abstract—Harmful algal blooms (HABs) pose significant threats to aquatic ecosystems, public health, and local economies by degrading water quality, causing fish kills, and producing harmful toxins. Traditional methods of detecting and mitigating HABs are often labor-intensive and expensive, targeting only smaller water bodies. Additionally, many detection systems currently work on a microbial scale or focus only on detection rather than classification. Existing research indicates that ultrasonic waves at specific frequencies can effectively destroy algal cells, but upscaling is necessary before implementation in the field becomes practical. We address this by leveraging machine learning to locate and classify multiple types of oceanic HABs and then outputting ultrasonic emissions at varied frequencies corresponding to each targeted HAB. The system analyzes satellite images with a convolutional neural network (CNN) to identify and categorize different types of harmful algae, allowing for rapid, large-scale monitoring of water bodies and providing timely data for environmental management. To train the CNN, we also construct a novel dataset containing 4998 satellite images of algal blooms along the west coast of North America. After the visual processing, we identify the optimal ultrasonic wave frequency for each identified HAB. Our model successfully identifies eight different algal genera with an accuracy of 98.2%. To tackle practical application, we propose a prototype to implement our machine learning model for algal classification with an ultrasonic irradiation device. It consists of two parts: a drone for autonomous scanning across the ocean, and an underwater device for treatment. Thus, we demonstrate the potential of machine learning to advance ultrasonic mitigation towards large-scale implementation.

Index Terms—oceanic ecosystems, harmful algal blooms, machine learning, satellite imagery, ultrasonic mitigation

I. INTRODUCTION

Harmful algal blooms (HABs) are occurring with increasing frequency in recent years due to climate change, causing widespread environmental, economic, and public health repercussions. HABs are responsible for the deaths of many species of aquatic and terrestrial organisms, including plants, fish, birds, mammals, and humans. A 2016 bloom of *Pseudochattonella* sp. in Chile killed 27 million salmon and trout [1], and over 67 reports of dogs poisoned by algal blooms were recorded in the US from 2007 to 2011 [2]. In addition, HABs

have a dramatic impact on the economy, due to relief and mitigation costs, as well as their effect on water-dependent industries. In aquaculture, for example, HABs can result in losses of 800 million dollars [3].

Given the threat that HABs pose, extensive research has gone into preventing bloom formation, but there is significantly less work in active treatment. Additionally, studies suggest that currently implemented treatments are largely ineffective with the exception of environmentally harmful chemical treatments [4]. Further, treatment efforts are targeted predominantly at freshwater HABs, neglecting oceanic blooms since they tend to be less prone to human contact.

One emerging method to address this gap is treatment through ultrasonic mitigation, motivated by the use of ultrasound in processing and extracting biological samples [5], [6]. The idea of using ultrasonic radiation to destroy algal cells was first implemented with a standing ultrasonic field at 1 MHz [7], and this has been refined in recent years towards ultrasonic irradiation at frequencies in the kilohertz range. However, existing research in ultrasonic mitigation occurs primarily in controlled laboratory settings, with very few pilot studies in the field [8]. Moreover, most studies observe the effect of ultrasound on a single species of algae, such as *M. aeruginosa* [9]–[11], or a very limited number of them [12], [13].

Many experiments considering multiple kinds of algae suggest that different algae are disrupted best by different ultrasonic frequencies, leading to data gathered on the optimal frequency to target certain freshwater algae [14], [15]. This suggests the potential of varying the emission frequency to upscale towards treating multiple kinds of algal blooms. However, before field testing of such a device can occur, more research on the scalability and applicability of ultrasonic mitigation is necessary [16].

Our research tackles these concerns by automating ultrasonic mitigation with machine learning and focusing on oceanic HABs, which are understudied with respect to ultrasonic mitigation. We propose a technique to support the ultrasonic mitigation of 8 different algal genera, exceeding the capacities presented in prior work. Our technique combines the mitigation output with scanning of the ocean using a

* Both authors contributed equally to this paper.

convolutional neural network (CNN) to locate HABs and identify the type of algae responsible for each one. In training the CNN, we compile our own HAB satellite images from the western coast of North America labeled by algal genus. This is because existing machine learning work involving aerial HAB data performs only detection or forecasting rather than algal classification, so the data is unlabeled, [17]–[19]. Finally, we further solidify the applicability of our approach, as well as ultrasonic mitigation as a whole, by discussing a prototype implementation.

Thus, the contributions of this research are:

- We collect and label a novel dataset of HAB satellite images, classified by algal genus, on the Pacific coast of North America (Section II).
- We train and evaluate a convolutional neural network for classifying HABs and outputting a prediction for the optimal ultrasonic emission frequency to treat them (Section III).
- We discuss an autonomous prototype to effectively integrate our model with the hardware necessary to emit ultrasonic radiation (Section IV).

II. DATASET

A. Image Collection

We began aggregating the dataset by locating HABs with corresponding time and genus data. The majority of historical records on HABs contain temporal data, but they do not identify the kind of algae causing the bloom. As a result, we decided to use the California Harmful Algal Bloom Monitoring and Alert Program (CALHABMAP), which reports genus concentrations from water samples taken periodically over multiple years, in combination with some records from the Harmful Algal Event Database (HAEDAT) [20] which contain genus information.

From these two sources, 8 well-documented bloom locations were chosen on the Pacific coast, ranging from British Columbia to Southern California. Many of these locations were chosen because they produced blooms during multiple years or from multiple genera, providing more extensive data. Location metadata is summarized in Table I. For each of the 8 locations, smaller sublocations were then selected to be visually monitored more carefully through satellite imagery.

Prior research involving satellite data of HABs has taken advantage of the Copernicus Sentinel-2 mission [21], [22], so we compiled our images from its publicly accessible API.

One particular feature utilized was the Ulyssys Water Quality Viewer (UQWV) [23], which processes spectral bands from Sentinel-2 that measure predicted chlorophyll and sediment concentration. UQWV attributes colors to various water qualities according to a two-dimensional color palette, where the two variables are the chlorophyll concentration and the sediment concentration.

The distinction between low water quality due to chlorophyll content versus that due to sediments is of key significance. This is because the difference between the two was

TABLE I
RECORDED GENERA AND BLOOM YEARS BY LOCATION.

Location	Genera	Collected Bloom Years
Clayoquot Sound	Chaetoceros, Dinophysis	2019
Georgia Strait	Dictyota	2018 - 2023
Del Norte coast	Alexandrium	2022, 2023
Bodega Bay	Pseudo-nitzschia	2021
Tomales Bay	Ceratium, Pseudo-nitzschia	2021
Richardson Bay	Heterosigma	2020 - 2022
Monterey Bay	Gymnodinium, Pseudo-nitzschia	2021
Ventura	Ceratium	2020, 2021

very difficult to determine visually, and to detect HABs, lots of chlorophyll but minimal sediments must be present. However, applying UQWV on a bloom obscures the color of the algae present, and color is a crucial feature for classifying algae. Therefore, for every sublocation being considered, we used true color images with their corresponding UQWV filtered images, as shown in Figure 1.

We analyzed the sublocations over predicted bloom events, manually identifying the time ranges when the blooms actually occurred with UQWV analysis. Then, for each sublocation, we randomly selected positions inside the sublocation boundary and took 256x256 pixel pictures (both true color and UQWV filtered versions) from these positions over the identified time ranges. Repeating this for every location and every sublocation inside of it completed the image gathering process, resulting in a raw dataset of 750 true color images and 750 filtered images. The data is distributed into equal orders of magnitude across algal genus, ranging from 57 to 199 images per genus.

B. Data Augmentation

Data augmentation with Keras’ ImageDataGenerator was used on the original dataset to ensure generalization of the machine learning model in every environmental condition and observation angle. This approach further enlarged the training data by injecting many transformations to simulate real-world variations which could be possible as a result of aerial imagery. The augmentations used include random rotations by up to 20°, since the test images could have been taken from several different angles, random width and height shifts by up to 20%, as well as positional distortions that could happen while acquiring satellite images.

All images were transformed by a shear by up to 20% of the viewing angle. It also performed random zooms of up to 20%, simulating different focal lengths of satellite observations. Horizontal flipping adds mirrored images, which allows the model to pick up symmetric patterns. In cases where these transformations create blank areas, it uses the nearest pixel value to fill the gaps without losing information on the images.

These augmentation techniques were applied to both the true color and filter images in the dataset. This process finalized the dataset to 4998 images, which was quite diverse and extensive for the model to train on, especially given the manual origin

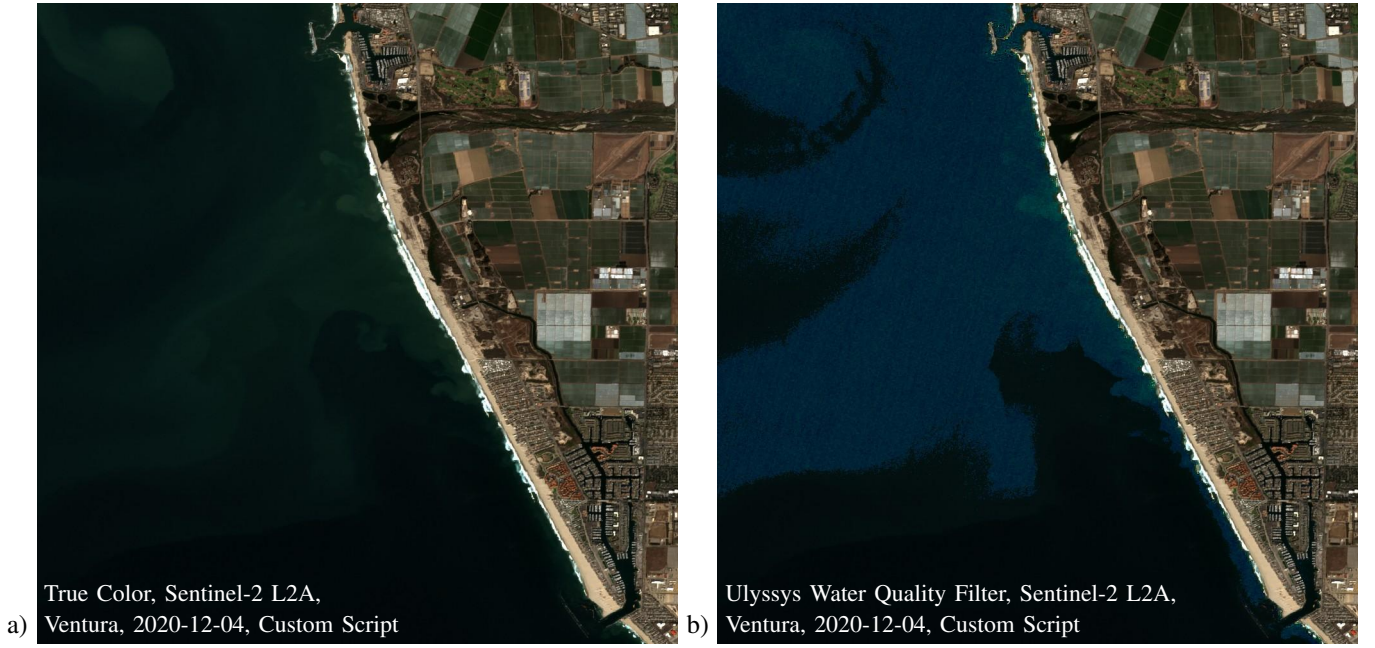


Fig. 1. True color (a) and UQWV-filtered (b) images of an HAB off the coast of Ventura, California

of the collection. By simulating real-world conditions under which satellite images can be taken from different angles and lighting, the model becomes more robust to new and heterogeneous data. The augmentation step was very critical in improving performance by preventing overfitting and increasing generalization to new unseen data to become more robust for the classification of different types of algae under varied conditions.

III. TECHNIQUE

A. Machine Learning Model

To classify the 8 different algae genera, a CNN was developed that utilized both true color satellite images and water quality filter images. The images used from the dataset were standardized at 256x256 pixels.

The CNN model architecture was developed to process both the true color images and water quality filter images concurrently in order to extract both visual and water quality features for accurate classification. Thus, two parallel branches are present in its structure, with one branch for each type of image input. The architecture of the model (see Figure 2) was such that it processes each kind of input independently and extracts features from them.

The first branch, which was used for processing the true color satellite images, comprises a set of convolutional layers aimed at capturing important visual features in the images, such as texture, shape, or color patterns, making it possible to distinguish between different kinds of algae. The filters of the convolutional layers were of increasing depth: 16 in the first layer, 64 in the second, and 128 in the last. All of the convolutional layers had a kernel size of 3x3, using the ReLU

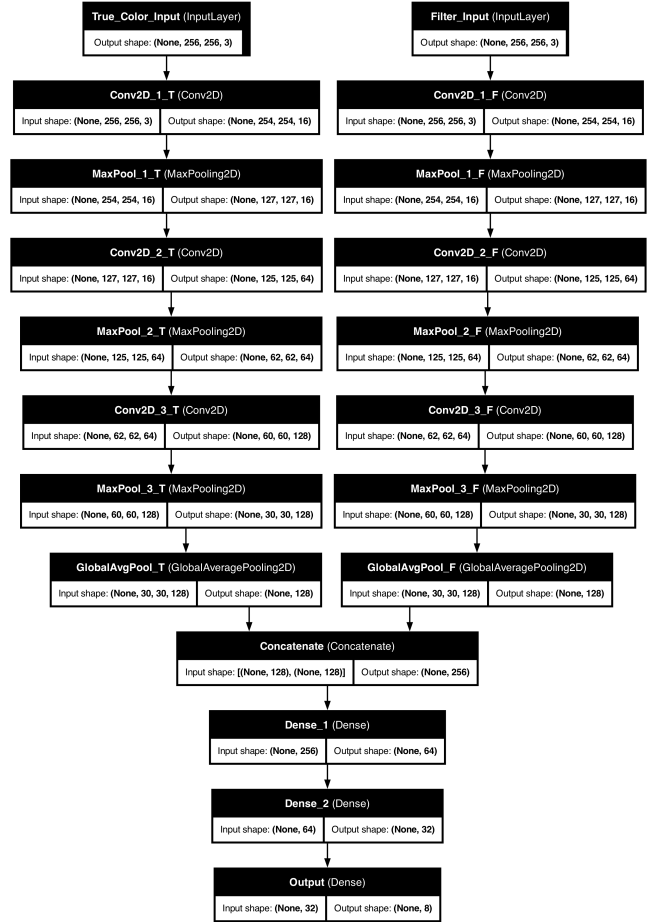


Fig. 2. CNN model architecture

activation function to incorporate non-linearity and help the model learn complex patterns by activating only positive feature responses. Max Pooling with a 2x2 pool size was applied after each convolutional layer to perform downsampling of the feature maps. Max Pooling reduces feature map dimensionality but still maintains the salient features that would guide the model's attention toward important information. This helps in preventing overfitting, and also computationally, it is very efficient. The last layers are Global Average Pooling applied over the feature maps. Unlike flattening the feature map, which results in many parameters, Global Average Pooling goes further to reduce each feature map to only one single value and hence dramatically decreases the number of parameters while preserving essential information on the image.

The second branch is similar in structure but was used exclusively to process water quality filter images. These images had significant additional context: the water quality indicators in the form of chlorophyll concentration or suspended matter, which allowed the model to identify algal presence much more accurately. The water quality filter branch was built in the same way as the true color branch: three convolutional layers, followed by Max Pooling and Global Average Pooling. Both branches possessed the same filter sizes and activations of the true color branch to make processing equivalent, even though the filtered images present different information.

After the features from both branches have been extracted and processed independently, the outputs of the two branches are concatenated into a single joint feature vector. This concatenation enables the model to take the visual and water quality aspects of the algae genera simultaneously in that data point, which provides a richer and more informative representation. The combined feature vector is passed through multiple fully connected layers to further enhance the feature representation and thereby prepare it for the final stage of classification. The fully connected layers start at 64 neurons, then followed by another layer of 32 neurons, all using ReLU activation. These layers further compress and refine the information taken from the convolutional layers, thereby making it more conducive to the final classification task. The size reduction of such fully connected layers is chosen to be most effective when balancing computation efficiency and accuracy, avoiding overfitting, and yet maintaining enough model capacity to predict well.

The last output layer is an 8-neuron layer, corresponding to the 8 genera of algae in the dataset. It uses a softmax activation to translate raw output into a probability distribution across classes. The softmax function compresses the output values between 0 and 1 and ensures that the probability for each class sums to 1. Therefore, the model predicts the genus with the highest probability, but it still takes into account the likelihood of other genera.

The model was run for 50 epochs at a learning rate of 0.001. To validate the model's effectiveness, we performed a 5-fold cross-validation on the augmented dataset of 4,998 images, calculating overall classification accuracy as well as per-genus accuracy. The careful structuring of two parallel branches for

TABLE II
OPTIMAL FREQUENCIES BY GENUS.

Species	Effective Ultrasound Frequency (kHz)
Alexandrium	25-30
Ceratium	30-60
Pseudo-nitzschia	50-100
Gymnodinium	30-60
Dityocystis	40-60
Chaetoceros	50-100
Dinophysis	30-50

two types of image processing allowed it to perceive both the visual and environmental features of algal blooms depicted in the two types of images.

B. Ultrasonic Treatment

Research has demonstrated that ultrasonic emission frequencies between 20 kHz and 100 kHz are most effective for treating HABs, with the specific optimal frequency range depending on the kind of algae. This frequency range is based on the physical characteristics of the algae in question, its response to hydrodynamic cavitation, and its cell wall composition.

Low-frequency ultrasound (20-30 kHz) is effective for softer cell walls, such as *Heterosigma* and *Alexandrium*, by creating large cavitation bubbles that disrupt cells [24]. Higher frequencies (50-100 kHz) are necessary for species with tougher silica-based cell walls, like *Pseudo-nitzschia* sp. and *Chaetoceros* sp., where smaller cavitation bubbles penetrate more rigid structures effectively [15]. *Ceratium* and *Gymnodinium*, two genera that tend to form large, dense blooms, have been effectively treated with frequencies ranging from 30 kHz to 60 kHz, where cavitation damages cell walls and disrupts their colonial structures [25]. The optimal frequency ranges for all 8 genera considered by the model are presented in Table II.

IV. HARDWARE INTEGRATION

This paper introduces a novel two-stage system to mitigate the impacts of HABs through algal-specific ultrasound frequencies. For this purpose, we propose a physical system in which there are two modules: an aerial drone for algal classification and an underwater drone with ultrasonic transducers for HAB treatment.

In its first stage, the developed system deploys an aerial drone fitted with imaging sensors and environmental-scanning equipment. The drone is intended to fly over affected water bodies and capture high-resolution images. It also collects relevant environmental data from the surface at which the algal bloom occurs. The drone will additionally gather contextual environmental data that may potentially affect the behavior of the bloom, like water temperature and turbidity.

Post-imaging, the drone classifies through the use of the CNN model the algal genera detected within the bloom. Proper identification is key to effectively treat the bloom because depending on the type of algae identified, there is an

optimal disruption frequency to emit. This module will query a database of optimal ultrasound frequencies for each algal genus that has been discussed in the earlier sections of this paper. Once the algae are identified, and thus the treatment frequency, the drone will communicate this information along with the GPS location of the bloom to the second module of the system.

The second component of the system includes an underwater device with ultrasonic emission capabilities. These transducers will deliver directed ultrasonic frequencies directly to the water in order to disrupt and neutralize the algae. Independently finding the GPS coordinates of the bloom, the underwater drone will target the frequency exposure outputted by the aerial drone. Once in position, the ultrasonic transducers will emit sound waves at the specified frequency. It functions based on ultrasonic-induced cavitation, where formation and collapse of microscopic bubbles cause local pressure changes that break down the cellular structure of the algae, effectively destroying them without the use of any chemicals.

This two-stage system allows non-invasive and precise HAB management. By combining genus-specific ultrasound treatment with the real-time detection of algae from the aerial images, the proposed solution can approach the problem of HABs in an effective way with minimal environmental disturbance. The modular design also makes it scalable, and hence applicable across large water bodies like the open ocean.

V. RESULTS AND DISCUSSION

The research contributes a novel dataset of HAB images, a CNN model for predicting the optimal ultrasonic emission frequency to target each HAB, and an integrated system with the necessary hardware to actively apply ultrasonic mitigation towards HABs.

The generated satellite image dataset of 4998 labeled images provides a diverse and comprehensive representation of HABs across multiple years, locations along the Pacific coast, and types of algae. It can be utilized in future studies which require aggregated HAB images.

The CNN model achieved high overall classification performance, with an overall accuracy of 98.2%, as well as F1-score, precision, and recall above 96.5%, in identifying the eight target genera of algae. Additionally, the accuracy by genus was above 95% for all genera. The use of data augmentation helped with preventing the model from overfitting. Additionally, the two CNN branches put together greatly improved model accuracy by providing the model with more context to make its prediction. These metrics underscore the CNN's strength in handling multi-class classification, although slight performance variations among genera indicate areas for model refinement.

There are a number of ways for further improvement of the system. The robustness in different regions can be increased by fine-tuning the CNN model to include more genera and environmental conditions. Furthermore, the system could continue to be optimized for large-scale deployment

by increasing image capture quality of the drone and the ultrasound transducers' depth-specific performance.

VI. CONCLUSION

The fusion of state-of-the-art machine learning with ultrasonic technology is a novel approach in HAB mitigation, promoting an environmentally friendly and scalable method of alleviating one of the pressing environmental challenges. This system has the potential to improve the environmental management of HABs. Genus-specific treatment is targeted and real-time, thereby reducing unintended impacts on surrounding ecosystems. With a model classification accuracy for algal genera of 98.2%, combined with targeted ultrasonic treatment, this technology showcases the potential for large-scale, chemical-free mitigation of HABs. This will not only address the ecological consequences caused by algal blooms but also set the groundwork for future advances in ecological monitoring and intervention, providing a sustainable path in solving related water quality issues.

REFERENCES

- [1] R. M. Montes, X. Rojas, P. Artacho, A. Tello, and R. A. Quiñones, "Quantifying harmful algal bloom thresholds for farmed salmon in southern Chile," *Harmful Algae*, vol. 77, pp. 55–65, Jul. 2018, doi: 10.1016/j.hal.2018.05.004.
- [2] L. C. Backer, J. H. Landsberg, M. Miller, K. Keel, and T. K. Taylor, "Canine cyanotoxin poisonings in the United States (1920s–2012): Review of suspected and confirmed cases from three data sources," *Toxins*, vol. 5, pp. 1597–1628, 2013, doi: 10.3390/toxins5091597.
- [3] P. Díaz-Tapia et al., "Impacts of harmful algal blooms on the aquaculture industry: Chile as a case study," *Perspectives in Phycology*, vol. 6, no. 1–2, Feb. 2019, doi: 10.1127/pip/2019/0081.
- [4] S. S. Anantapantula and A. E. Wilson, "Most treatments to control freshwater algal blooms are not effective: Meta-analysis of field experiments," *Water Res.*, vol. 243, 2023, Art. no. 120342, doi: 10.1016/j.watres.2023.120342.
- [5] M. D. Esclapez, J. V. García-Pérez, A. Mulet, and J. A. Cárcel, "Ultrasound-assisted extraction of natural products," *Food Eng. Rev.*, vol. 3, pp. 108–120, 2011, doi: 10.1007/s12393-011-9036-6.
- [6] T. Furuki, S. Maeda, S. Imajo, et al., "Rapid and selective extraction of phycocyanin from *Spirulina platensis* with ultrasonic cell disruption," *J. Appl. Phycol.*, vol. 15, pp. 319–324, 2003.
- [7] D. L. Miller, "Effects of a high-amplitude 1-MHz standing ultrasonic field on the algae *Hydrodictyon*," *IEEE Trans. Ultrason., Ferroelectr., Freq. Control*, vol. 33, no. 2, pp. 165–170, March 1986, doi: 10.1109/T-UFFC.1986.26810.
- [8] X. Wu, E. M. Joyce, and T. J. Mason, "The effects of ultrasound on cyanobacteria," *Harmful Algae*, vol. 10, no. 6, pp. 738–743, 2011.
- [9] G. Zhang, P. Zhang, B. Wang, and H. Liu, "Ultrasonic frequency effects on the removal of *Microcystis aeruginosa*," *Ultrason. Sonochem.*, vol. 13, no. 5, pp. 446–450, 2006.
- [10] G. Zhang, P. Zhang, and M. Fan, "Ultrasound-enhanced coagulation for *Microcystis aeruginosa* removal," *Ultrason. Sonochem.*, vol. 16, no. 3, pp. 334–338, 2009.
- [11] B. Ma, Y. Chen, H. Hao, M. Wu, B. Wang, H. Lv, and G. Zhang, "Influence of ultrasonic field on microcystins produced by bloom-forming algae," *Colloids Surf. B: Biointerfaces*, vol. 41, no. 2–3, pp. 197–201, 2005.
- [12] P. M. King, K. Nowotarski, E. M. Joyce, and T. J. Mason, "Ultrasonic disruption of algae cells," in *Int. Congr. Ultrasonics: Gdańsk 2011*, vol. 1433, no. 1, pp. 237–240, 2012, doi: 10.1063/1.3703179.
- [13] P. Rajasekhar, L. Fan, T. Nguyen, and F. A. Roddick, "Impact of sonication at 20 kHz on *Microcystis aeruginosa*, *Anabaena circinalis*, and *Chlorella* sp.," *Water Res.*, vol. 46, no. 5, pp. 1473–1481, 2012.
- [14] M. Kurokawa, P. M. King, X. Wu, E. M. Joyce, T. J. Mason, and K. Yamamoto, "Effect of sonication frequency on the disruption of algae," *Ultrason. Sonochem.*, vol. 31, pp. 157–162, 2016.

- [15] X. Wu and T. J. Mason, "Evaluation of power ultrasonic effects on algae cells at a small pilot scale," *Water*, vol. 9, no. 7, Art. no. 470, 2017, doi: 10.3390/w9070470.
- [16] J. Park, J. Church, Y. Son, K.-T. Kim, and W. H. Lee, "Recent advances in ultrasonic treatment: Challenges and field applications for controlling harmful algal blooms (HABs)," *Ultrason. Sonochem.*, vol. 38, pp. 326–334, 2017.
- [17] P. Yu, R. Gao, D. Zhang, and Z.-P. Liu, "Predicting coastal algal blooms with environmental factors by machine learning methods," *Ecol. Indic.*, vol. 123, 2021, Art. no. 107334, doi: 10.1016/j.ecolind.2020.107334.
- [18] M. Zahir et al., "A review on monitoring, forecasting, and early warning of harmful algal bloom," *Aquaculture*, vol. 593, 2024, Art. no. 741351, doi: 10.1016/j.aquaculture.2024.741351.
- [19] Y. Yao, et al., "Detection of *Karenia brevis* red tides on the West Florida Shelf using VIIRS observations: Accounting for spatial coherence with artificial intelligence," *Remote Sensing of Environment*, vol. 298, 2023.
- [20] Intergovernmental Oceanographic Commission of UNESCO (2021). Harmful Algae Event Database (HAEDAT). <http://haedat.iode.org>
- [21] M. H. Khalili and M. Hasanlou, "Harmful algal blooms monitoring using Sentinel-2 satellite images," *Int. Arch. Photogramm. Remote Sens. Spatial Inf. Sci.*, vol. XLII-4/W18, pp. 609–613, 2019, doi: 10.5194/isprs-archives-XLII-4-W18-609-2019.
- [22] D. Xu, Y. Pu, M. Zhu, Z. Luan, and K. Shi, "Automatic detection of algal blooms using Sentinel-2 MSI and Landsat OLI images," *IEEE J. Sel. Top. Appl. Earth Obs. Remote Sens.*, vol. 14, pp. 8497–8511, 2021, doi: 10.1109/JSTARS.2021.3105746.
- [23] A. Zlinszky and G. Padányi-Gulyás, "Ulyssys Water Quality Viewer Technical Description Supplementary," 2020, doi: 10.20944/preprints202001.0386.v1.
- [24] A. Sukenik and A. Kaplan, "Cyanobacterial harmful algal blooms in aquatic ecosystems: A comprehensive outlook on current and emerging mitigation and control approaches," *Microorganisms*, vol. 9, no. 7, Art. no. 1472, Jul. 2021, doi: 10.3390/microorganisms9071472.
- [25] K. Nakano, T. J. Lee, and M. Matsumura, "In situ algal bloom control by the integration of ultrasonic radiation and jet circulation to flushing," *Environ. Sci. Technol.*, vol. 35, no. 24, pp. 4941–4946, 2001, doi: 10.1021/es010711c.